# Supplemental Material: Asymptotical Locking Tomography of High-Dimensional Entanglement

Ling-Jun Kong(孔令军),[1,2] Rui Liu(刘瑞),[3] Wen-Rong Qi(齐文荣),[3] Zhou-Xiang Wang(王周祥),[3]
Shuang-Yin Huang(黄双印),[3] Chenghou Tu(涂成厚),[3] Yongnan Li(李勇男),[3,*] and Hui-Tian Wang(王慧田)[1,2,†]

[1]*National Laboratory of Solid State Microstructures, Nanjing University, Nanjing 210093, China*
[2]*Collaborative Innovation Center of Advanced Microstructures, Nanjing University, Nanjing 210093, China*
[3]*Key Laboratory of Weak-Light Nonlinear Photonics and School of Physics, Nankai University, Tianjin 300071, China*

## I. CRITERION SEARCHING FOR THE SUITABLE TRANSFORMATION MATRIX

As described in the main text, the criterion matrix **C** defined as

$$C_{kl} = \left| \sum_{m=1}^{d} \lambda_m \widetilde{T}^{\dagger}_{mk} \widetilde{T}^{\dagger}_{ml} e^{i\beta_m} \right|^2. \tag{S1}$$

The criterion is defined as

$$\mathbf{C}(\widetilde{\mathbf{T}}, \{\beta_m\}) = \mathbf{C}(\widetilde{\mathbf{T}}, \{\beta'_m\}), \quad \text{iff } \{\beta_m\} = \{\beta'_m\}. \tag{S2}$$

In the processing of experimental data, a program with the two-fold nested loops ($\widetilde{\mathbf{T}}$ as the outer loop and $\{\beta_m\}$ as the inner loop, as shown in Fig. S1) can be used to search for the suitable transformation matrix **T**.

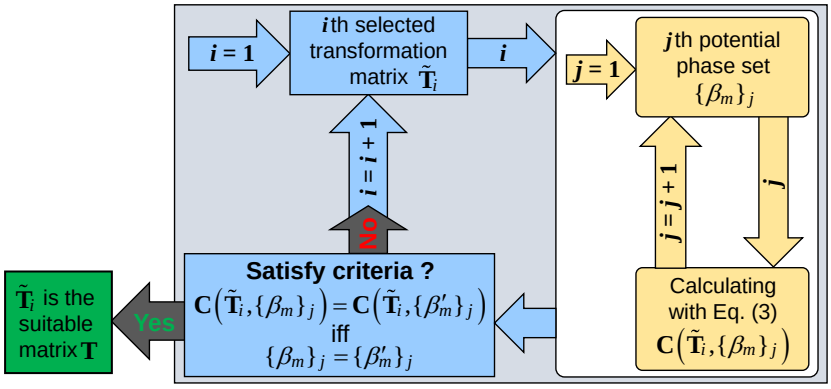


FIG. S1: Schematic of searching for the suitable transformation matrix with the criterion.

## II. PROJECTION OF THE TWO BASES IN OUR 4-DIMENSIONAL ENTANGLEMENT

In our 4-dimensional entanglement experiment, the global basis are $|\nu_1\rangle = |H,+1\rangle$, $|\nu_2\rangle = |V,+1\rangle$, $|\nu_3\rangle = |V,-1\rangle$, and $|\nu_4\rangle = |H,-1\rangle$. For the intended target states $|\Phi_1\rangle$ in the main text and $|\Phi_3\rangle$ in Section S3, the first basis of photon-$A$ are defined as $|\phi^A_m\rangle = |\nu_m\rangle$ ($m = 1,2,3,4$), while the first basis of photon-$B$ are defined as $|\phi^B_1\rangle = |\nu_4\rangle$, $|\phi^B_2\rangle = |\nu_3\rangle$, $|\phi^B_3\rangle = |\nu_2\rangle$, $|\phi^B_4\rangle = |\nu_1\rangle$. For the intended target states $|\Phi_2\rangle$ in the main text and $|\Phi_4\rangle$ in Section S3, the first basis of photon-$A$ are defined as $|\phi^A_m\rangle = |\nu_m\rangle$, while the first basis of photon-$B$ are defined as $|\phi^B_1\rangle = |\nu_3\rangle$, $|\phi^B_2\rangle = |\nu_4\rangle$, $|\phi^B_3\rangle = |\nu_1\rangle$, $|\phi^B_4\rangle = |\nu_2\rangle$. The second basis are defined as

*Electronic address: liyongnan@nankai.edu.cn
†Electronic address: htwang@nju.edu.cn

$$|\varphi_1^X\rangle = (+|\phi_1^X\rangle + |\phi_2^X\rangle + |\phi_3^X\rangle - |\phi_4^X\rangle)/2, \tag{S3a}$$
$$|\varphi_2^X\rangle = (+|\phi_1^X\rangle + |\phi_2^X\rangle - |\phi_3^X\rangle + |\phi_4^X\rangle)/2, \tag{S3b}$$
$$|\varphi_3^X\rangle = (+|\phi_1^X\rangle - |\phi_2^X\rangle + |\phi_3^X\rangle + |\phi_4^X\rangle)/2, \tag{S3c}$$
$$|\varphi_4^X\rangle = (-|\phi_1^X\rangle + |\phi_2^X\rangle + |\phi_3^X\rangle + |\phi_4^X\rangle)/2, \tag{S3d}$$

where $X = A$ or $B$. As an example, photons in the states $|\phi_1^A\rangle$ and $|\varphi_1^A\rangle$ can be projected with post-selection by using HWP1, QWP1, 1/2-order $q$-plate, QWP2, HWP2, PBS, lens, and SMF in turn (as shown in Row-3 of Fig. S2, where QWP—quarter wave plate, HWP—half wave plate, PBS—polarizing beam splitter). Row-1 illustrates the projective evolution from $|\phi_1^A\rangle = |\nu_1\rangle = |H,+1\rangle$ to $|H,0\rangle$ through a series of operations (HWP1@0°, QWP1@−45°, $q$-plate, QWP2@−45°, and HWP2@0° in turn) in Row-2. Row-5 shows the projective evolution of $|\varphi_1^A\rangle \propto |H,+1\rangle + |V,+1\rangle + |V,-1\rangle - |H,-1\rangle$ by the operations in Row-4. When setting HWP1@+22.5° and QWP1@−45°, $|\varphi_1^A\rangle \Rightarrow |L,+1\rangle - |R,-1\rangle$, which is finally converted into $|H,0\rangle$ by the $q$-plate, QWP2@−45° and HWP2@−22.5°. After passing through PBS, $|H,0\rangle$ is coupled into a SMF and detected.

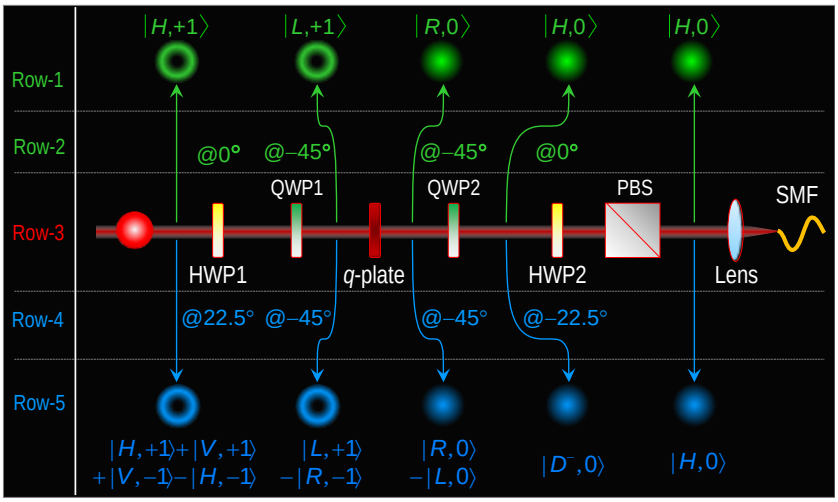


FIG. S2: Procedures of projection measurement for the first basis $|\phi_1^A\rangle$ and second basis $|\varphi_1^A\rangle$. Row-3 shows the optical elements required for projective measurement, HWP1, QWP1, $q$-plate, QWP2, HWP2, PBS, lens, and SMF in turn. Row-1 shows the evolutions of $|\phi_1^A\rangle = |H,+1\rangle$ by operations in Row-2. Row-5 shows evolutions of $|\varphi_1^A\rangle \propto |H,+1\rangle + |V,+1\rangle + |V,-1\rangle - |H,-1\rangle$ by operations in Row-4.

In fact, the procedures of projection measurement, as shown in Fig. S2, are suitable for all the first basis $\{|\phi_m^{A/B}\rangle\}$ and all the second basis $\{|\varphi_m^{A/B}\rangle\}$ ($m = 1,2,3,4$). The detailed evolutions of all the basis for photon-$A$ are described as

$$|\phi_1^A\rangle = |H,+1\rangle \xrightarrow{\text{HWP1@0°}} |H,+1\rangle \xrightarrow{\text{QWP1@−45°}} |L,+1\rangle \xrightarrow{q\text{−plate1}} |R,0\rangle \xrightarrow{\text{QWP2@−45°}} |H,0\rangle \xrightarrow{\text{HWP2@0°}} |H,0\rangle \tag{S4a}$$
$$|\phi_2^A\rangle = |V,+1\rangle \xrightarrow{\text{HWP1@0°}} |V,+1\rangle \xrightarrow{\text{QWP1@+45°}} |L,+1\rangle \xrightarrow{q\text{−plate1}} |R,0\rangle \xrightarrow{\text{QWP2@−45°}} |H,0\rangle \xrightarrow{\text{HWP2@0°}} |H,0\rangle \tag{S4b}$$
$$|\phi_3^A\rangle = |V,-1\rangle \xrightarrow{\text{HWP1@0°}} |V,-1\rangle \xrightarrow{\text{QWP1@−45°}} |R,-1\rangle \xrightarrow{q\text{−plate1}} |L,0\rangle \xrightarrow{\text{QWP2@+45°}} |H,0\rangle \xrightarrow{\text{HWP2@0°}} |H,0\rangle. \tag{S4c}$$
$$|\phi_4^A\rangle = |H,-1\rangle \xrightarrow{\text{HWP1@0°}} |H,-1\rangle \xrightarrow{\text{QWP1@+45°}} |R,-1\rangle \xrightarrow{q\text{−plate1}} |L,0\rangle \xrightarrow{\text{QWP2@+45°}} |H,0\rangle \xrightarrow{\text{HWP2@0°}} |H,0\rangle \tag{S4d}$$
$$\begin{aligned}|\varphi_1^A\rangle \propto |H,+1\rangle + |V,+1\rangle + |V,-1\rangle - |H,-1\rangle \propto |D^+,+1\rangle - |D^-,-1\rangle \xrightarrow{\text{HWP1@+22.5°}} |H,+1\rangle - |V,-1\rangle \\ \xrightarrow{\text{QWP1@−45°}} |L,+1\rangle - |R,-1\rangle \xrightarrow{q\text{−plate}} |R,0\rangle - |L,0\rangle \xrightarrow{\text{QWP2@−45°}} |D^-,0\rangle \xrightarrow{\text{HWP2@−22.5°}} |H,0\rangle\end{aligned} \tag{S4e}$$
$$\begin{aligned}|\varphi_2^A\rangle \propto |H,+1\rangle + |V,+1\rangle - |V,-1\rangle + |H,-1\rangle \propto |D^+,+1\rangle + |D^-,-1\rangle \xrightarrow{\text{HWP1@+22.5°}} |H,+1\rangle + |V,-1\rangle \\ \xrightarrow{\text{QWP1@−45°}} |L,+1\rangle + |R,-1\rangle \xrightarrow{q\text{−plate}} |R,0\rangle + |L,0\rangle \xrightarrow{\text{QWP2@−45°}} |D^+,0\rangle \xrightarrow{\text{HWP2@+22.5°}} |H,0\rangle\end{aligned} \tag{S4f}$$
$$\begin{aligned}|\varphi_3^A\rangle \propto |H,+1\rangle - |V,+1\rangle + |V,-1\rangle + |H,-1\rangle \propto |D^-,+1\rangle + |D^+,-1\rangle \xrightarrow{\text{HWP1@+22.5°}} |V,+1\rangle + |H,-1\rangle \\ \xrightarrow{\text{QWP1@+45°}} |L,+1\rangle + |R,-1\rangle \xrightarrow{q\text{−plate}} |R,0\rangle + |L,0\rangle \xrightarrow{\text{QWP2@−45°}} |D^+,0\rangle \xrightarrow{\text{HWP2@+22.5°}} |H,0\rangle\end{aligned} \tag{S4g}$$

$$|\varphi_4^A\rangle \propto -|H,+1\rangle + |V,+1\rangle + |V,-1\rangle + |H,-1\rangle \propto |D^-,+1\rangle - |D^+,-1\rangle \xrightarrow{\text{HWP1@}+22.5^\circ} |V,+1\rangle - |H,-1\rangle$$
$$\xrightarrow{\text{QWP1@}+45^\circ} |L,+1\rangle - |R,-1\rangle \xrightarrow{q\text{-plate}} |R,0\rangle - |L,0\rangle \xrightarrow{\text{QWP2@}-45^\circ} |D^-,0\rangle \xrightarrow{\text{HWP2@}-22.5^\circ} |H,0\rangle. \tag{S4h}$$

Here $|R\rangle = (|H\rangle + j|V\rangle)/\sqrt{2}$ and $|L\rangle = (|H\rangle - j|V\rangle)/\sqrt{2}$ represent right and left circularly polarized states, respectively. $|D^\pm\rangle = (|H\rangle \pm |V\rangle)/\sqrt{2}$. The state $|H,0\rangle$ can be coupled into a single mode fiber. Similarly, the detailed evolutions of all the basis for photon-$B$ are easily obtained by Eq. (S4) with the aid of Eq. (S3).

## III. EXPERIMENTAL RESULTS FOR OTHER TWO 4-DIMENSIONAL HYPERENTANGLED STATES

In the main text, our ALT method has been applied to test the spin-OAM hyperentangled states $|\Phi_1\rangle \propto (|H^A\rangle|H^B\rangle + |V^A\rangle|V^B\rangle) \otimes |+1^A\rangle|-1^B\rangle + |-1^A\rangle|+1^B\rangle$ and $|\Phi_2\rangle \propto (|H^A\rangle|V^B\rangle - |V^A\rangle|H^B\rangle) \otimes |+1^A\rangle|-1^B\rangle + |-1^A\rangle|+1^B\rangle$ (see Fig. 2 in the main text). Here,

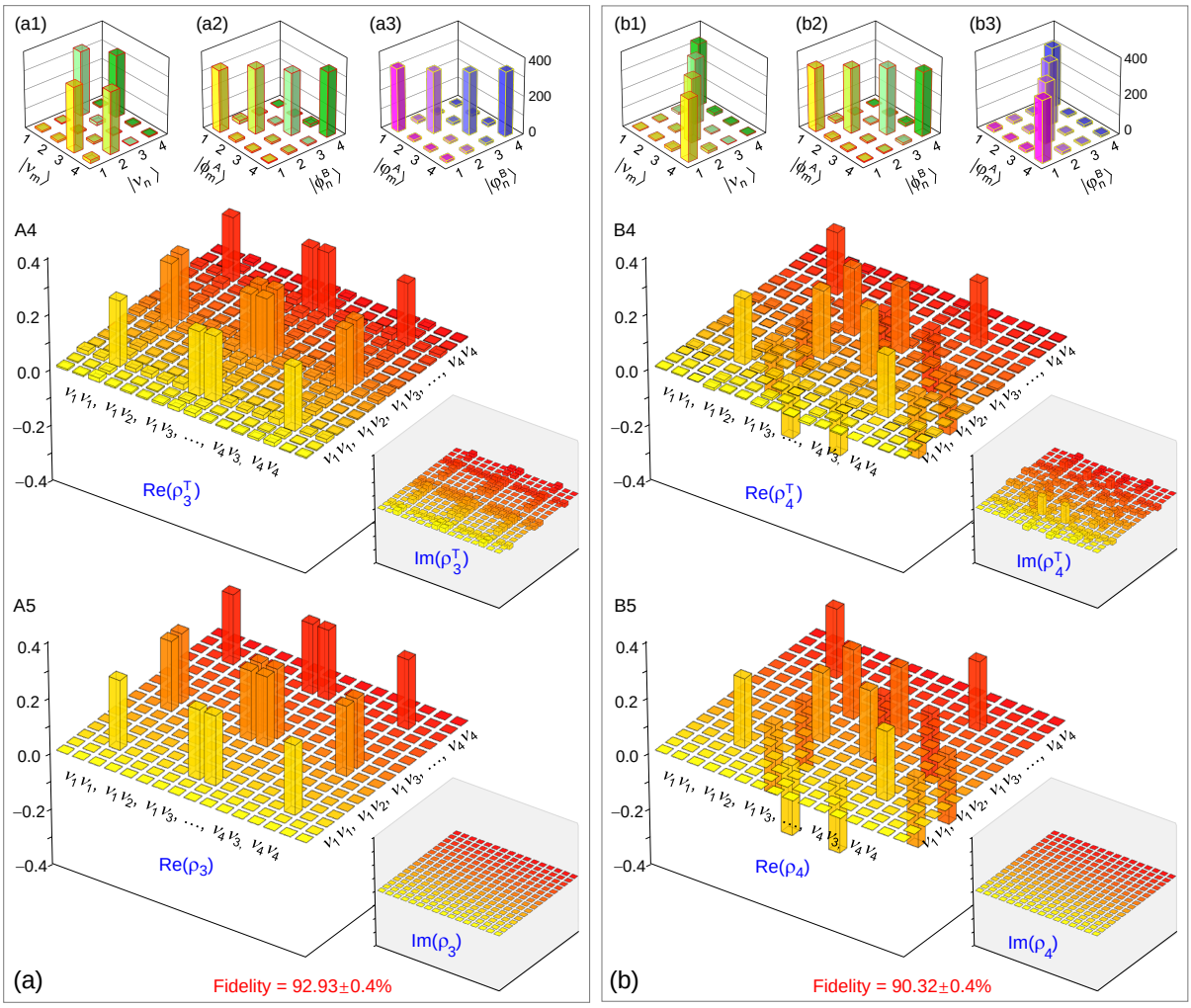


FIG. S3: Experimental data and reconstructed density matrices for the spin-OAM hyperentangled states. (a) Spin-OAM hyperentangled state $|\Phi_3\rangle$. (b) Spin-OAM hyperentangled state $|\Phi_4\rangle$. Two-photon coincidence counts for the intended target state $|\Phi_3\rangle$ under the global product basis of (a1) $\{|\nu_m\rangle|\nu_n\rangle\}$, (a2) the first basis $\{|\phi_m^A\rangle|\phi_n^B\rangle\}$, and (a3) the second basis $\{|\varphi_m^A\rangle|\varphi_n^B\rangle\}$. Coincidence counts $\mathbf{N}'$ in (a2) come directly from (a1) by defining the first basis as $|\phi_1^A\rangle = |\nu_1\rangle$, $|\phi_2^A\rangle = |\nu_2\rangle$, $|\phi_3^A\rangle = |\nu_3\rangle$, $|\phi_4^A\rangle = |\nu_4\rangle$; $|\phi_1^B\rangle = |\nu_3\rangle$, $|\phi_2^B\rangle = |\nu_4\rangle$, $|\phi_3^B\rangle = |\nu_1\rangle$, $|\phi_4^B\rangle = |\nu_2\rangle$. Experimentally and theoretically reconstructed density matrices, $\rho_3^T = |\Phi_3^T\rangle\langle\Phi_3^T|$ and $\rho_3 = |\Phi_3\rangle\langle\Phi_3|$ in (a4) in (a5), respectively. Similar to (a1)-(a5), (b1)-(b5) show results for the intended target state $|\Phi_4\rangle$. Coincidence counts $\mathbf{N}'$ in (b2) come directly from (b1) by defining the first basis as $|\phi_1^A\rangle = |\nu_1\rangle$, $|\phi_2^A\rangle = |\nu_2\rangle$, $|\phi_3^A\rangle = |\nu_3\rangle$, $|\phi_4^A\rangle = |\nu_4\rangle$; $|\phi_1^B\rangle = |\nu_4\rangle$, $|\phi_2^B\rangle = |\nu_3\rangle$, $|\phi_3^B\rangle = |\nu_2\rangle$, $|\phi_4^B\rangle = |\nu_1\rangle$. Experimentally reconstructed density matrix $\rho_4^T = |\Phi_4^T\rangle\langle\Phi_4^T|$ in (b4).

the experimental results with our ALT method for the states $|\Phi_3\rangle \propto (|H^A\rangle|V^B\rangle + |V^A\rangle|H^B\rangle) \otimes |+1^A\rangle|-1^B\rangle + |-1^A\rangle|+1^B\rangle$ and $|\Phi_4\rangle \propto (|H^A\rangle|H^B\rangle - |V^A\rangle|V^B\rangle) \otimes |+1^A\rangle|-1^B\rangle + |-1^A\rangle|+1^B\rangle$ are shown in Figs. S3A and S3B, respectively. All these experimental data demonstrates the feasibility of our ALT method.

## IV. GUIDE FOR OPTIMIZING THE STATE GENERATED IN LAB

The result of tomography can be used to diagnose the deviation of the prepared state from our intended target one. More importantly, the result of tomography is also able to give a reference for optimizing the prepared state, making it closer to our intended target state. Here, we show an example to describe this procedure.

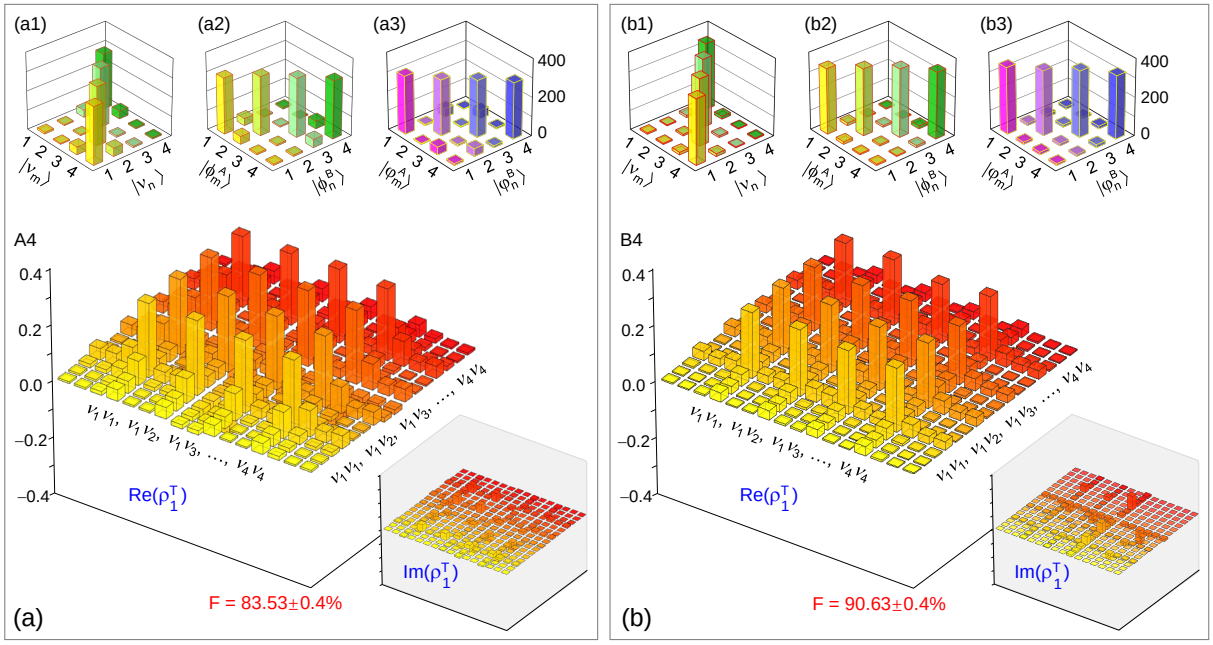


FIG. S4: Optimizing the state generated in lab. (a) and (b) show the tomography results of the states generated in the lab before and after the fine adjustment, respectively. Coincidence counts under the global basis $\{|\nu_m\rangle|\nu_n\rangle\}$ in (a1) and (b1), the first basis $\{|\phi_m^A\rangle|\phi_n^B\rangle\}$ in (a2) and (b2), and the second basis $\{|\varphi_m^A\rangle|\varphi_n^B\rangle\}$ in (a3) and (b3) for the intended target state $|\Phi_1\rangle$. Coincidence counts $\mathbf{N}'$ in (a2) and (b2) come from (a1) and (b1), by defining the first base as $|\phi_m^A\rangle = |\nu_m\rangle$, $|\phi_1^B\rangle = |\nu_4\rangle$, $|\phi_2^B\rangle = |\nu_3\rangle$, $|\phi_3^B\rangle = |\nu_2\rangle$ and $|\phi_4^B\rangle = |\nu_1\rangle$, respectively. (a4) and (b4) show the real and image parts of the experimentally reconstructed density matrix $\rho_1^T = |\Phi_1^T\rangle\langle\Phi_1^T|$, respectively. The fidelity of the state before (after) the fine adjustment is $F = 83.53 \pm 0.4\%$ ($90.63 \pm 0.4\%$).

For the 4-dimensional spin-OAM hyperentangled state (see the main text), the global basis are $|\nu_1\rangle = |H,+1\rangle$, $|\nu_2\rangle = |H,-1\rangle$, $|\nu_3\rangle = |V,+1\rangle$, and $|\nu_4\rangle = |V,-1\rangle$. For the intended target states $|\Phi_1\rangle \propto (|H^A\rangle|H^B\rangle + |V^A\rangle|V^B\rangle) \otimes (|+1^A\rangle|-1^B\rangle + |-1^A\rangle|+1^B\rangle)$, the first basis are defined as $|\phi_m^A\rangle = |\nu_m\rangle$, $|\phi_1^B\rangle = |\nu_4\rangle$, $|\phi_2^B\rangle = |\nu_3\rangle$, $|\phi_3^B\rangle = |\nu_2\rangle$, and $|\phi_4^B\rangle = |\nu_1\rangle$. In experiment, we firstly prepare a state and then carry out the tomography measurement result as shown in Fig. S4A, the detected state can be written as

$$\begin{aligned}
|\Phi_1^T\rangle = &+ 0.4601|\phi_1^A\rangle|\phi_1^B\rangle + 0.1677e^{2.8908i}|\phi_1^A\rangle|\phi_2^B\rangle + 0.0593|\phi_1^A\rangle|\phi_3^B\rangle + 0.0796|\phi_1^A\rangle|\phi_4^B\rangle \\
&+ 0.1739e^{-0.5232i}|\phi_2^A\rangle|\phi_1^B\rangle + 0.4639e^{-0.0030i}|\phi_2^A\rangle|\phi_2^B\rangle + 0.0650|\phi_2^A\rangle|\phi_3^B\rangle + 0.0650|\phi_2^A\rangle|\phi_4^B\rangle \\
&+ 0.0750|\phi_3^A\rangle|\phi_1^B\rangle + 0.0750|\phi_3^A\rangle|\phi_2^B\rangle + 0.4646e^{-0.2384i}|\phi_3^A\rangle|\phi_3^B\rangle + 0.1613e^{-0.0552i}|\phi_3^A\rangle|\phi_4^B\rangle \\
&+ 0.0702|\phi_4^A\rangle|\phi_1^B\rangle + 0.0702|\phi_4^A\rangle|\phi_2^B\rangle + 0.1698e^{3.1084i}|\phi_4^A\rangle|\phi_3^B\rangle + 0.4524e^{-0.2412i}|\phi_4^A\rangle|\phi_4^B\rangle \\
\approx &+ 0.92|\Phi_1\rangle - 0.33|\Phi_2\rangle + 0.21|\text{Noise}\rangle. \qquad \text{(S5)}
\end{aligned}$$

The fidelity of $|\Phi_1^T\rangle$ with respect to $|\Phi_1\rangle$, can be calculated as $F(\Phi_1, \Phi_1^T) = \text{Tr}\{(|\Phi_1\rangle\langle\Phi_1|)(|\Phi_1^T\rangle\langle\Phi_1^T|)\} = 83.53\%$, meaning that the prepared state has a deviation from the intended target state. However, the tomography result can give us a guide how to adjust the optical elements used in experiment, making $|\Phi_1^T\rangle$ closer to $|\Phi_1\rangle$. By analyzing Eq. (S5), we find that the fidelity can

be improved by the operations $|\phi_1^A\rangle \to \cos\alpha|\phi_1^A\rangle + \sin\alpha|\phi_2^A\rangle$, $|\phi_2^A\rangle \to \cos\alpha|\phi_2^A\rangle - \sin\alpha|\phi_1^A\rangle$, $|\phi_3^A\rangle \to \cos\alpha|\phi_3^A\rangle - \sin\alpha|\phi_4^A\rangle$, and $|\phi_4^A\rangle \to \cos\alpha|\phi_4^A\rangle + \sin\alpha|\phi_3^A\rangle$, which can be realized by fine adjusting the orientation of HWP in path-A (Fig. 1 of the main text). In principle, when $\alpha = -15.12°$, the fidelity can be raised to $F = 93.70\%$. In our experiment, the tomography result of the improved state is shown in Fig. S4B, the fidelity is experimentally improved to 90.63%, which is slightly lower than 93.70%, due to the imperfections in the optical elements, alignment, and so on.

## V. DETAILS FOR ACQUIRING PHASE INFORMATION

We give the detail for acquiring phase information of the intended target state in our experiment. As stated in the main text, after measuring the coincidence counts matrix $\mathbf{N}'$ under the first product basis $\{|\phi_m^A\rangle|\phi_n^B\rangle\}$, we write the preliminary result of tomography for the state generated in the lab as $|\Phi_1^T\rangle = \sum_{m=1}^4 \lambda_m e^{i\theta_m}|\phi_m^A\rangle|\phi_m^B\rangle$, where $\lambda_m = \sqrt{N'_m/\sum_m N'_m}$ and $N'_m$ is a diagonal element of $\mathbf{N}'$. Following the criterion in Eq. (4) of the main text, we find a suitable transformation matrix $\mathbf{T}$

$$\mathbf{T} = \frac{1}{2}\begin{bmatrix} 1 & 1 & 1 & -1 \\ 1 & 1 & -1 & 1 \\ 1 & -1 & 1 & 1 \\ -1 & 1 & 1 & 1 \end{bmatrix}. \tag{S6}$$

We easily construct the second basis $\{|\varphi_m^X\rangle\}$ $(X = A, B)$ by Eq. (5) in the main text. Then we measure the coincidence counts matrix $\mathbf{N}''$ under the second product basis $\{|\varphi_m^A\rangle|\varphi_n^B\rangle\}$. Due to the symmetry of $\mathbf{N}''$, we need only to measure the independent elements of $N''_{mn}|_{m\le n}$ in experiment. We build from Eq. (6) in the main text a set of nonlinear equations as

$$1 + 2\lambda_1\lambda_2\cos\delta_{12} + 2\lambda_1\lambda_3\cos\delta_{13} + 2\lambda_1\lambda_4\cos\delta_{14} + 2\lambda_2\lambda_3\cos\delta_{23} + 2\lambda_2\lambda_4\cos\delta_{24} + 2\lambda_3\lambda_4\cos\delta_{34} = N''_{11}/N''_{\mathrm{C}}, \tag{S7a}$$

$$1 + 2\lambda_1\lambda_2\cos\delta_{12} - 2\lambda_1\lambda_3\cos\delta_{13} - 2\lambda_1\lambda_4\cos\delta_{14} - 2\lambda_2\lambda_3\cos\delta_{23} - 2\lambda_2\lambda_4\cos\delta_{24} + 2\lambda_3\lambda_4\cos\delta_{34} = N''_{12}/N''_{\mathrm{C}}, \tag{S7b}$$

$$1 - 2\lambda_1\lambda_2\cos\delta_{12} + 2\lambda_1\lambda_3\cos\delta_{13} - 2\lambda_1\lambda_4\cos\delta_{14} - 2\lambda_2\lambda_3\cos\delta_{23} + 2\lambda_2\lambda_4\cos\delta_{24} - 2\lambda_3\lambda_4\cos\delta_{34} = N''_{13}/N''_{\mathrm{C}}, \tag{S7c}$$

where $N''_{\mathrm{C}} = (2N''_{11} + N''_{12} + N''_{13} + N''_{14} + N''_{23} + N''_{24} + N''_{34})/8$ is a normalized coefficient and $\delta_{mn} = \theta_n - \theta_m$. The phase information of the target state $|\Phi\rangle$ is contained in the relative phase differences $\{0 \le \delta_{1n} \le \pi\}_{n=2,3,4}$, which can be calculated from Eq. (S7).

## VI. AN EXAMPLE FOR TOMOGRAPHY BY USING OUR ALT METHOD

Without loss of generality, let us consider an unknown 5-dimensional bipartite state. In order to have a general understanding of the unknown state, we carry out 25 local projective measurements under the first global product basis $\{|\phi_m^A\rangle|\phi_n^B\rangle\}$ to obtain the coincidence counts matrix $\mathbf{N}'$. The element of the normalized coefficient matrix, $\lambda_{mn}$, can be written as $\lambda_{mn} = \sqrt{\langle\phi_m^A|\langle\phi_n^B|\rho|\phi_m^A\rangle|\phi_n^B\rangle} = \sqrt{N'_{mn}/\sum_{m,n} N'_{mn}}$. If the first basis is well selected, the number of nonzero $\lambda_{mn}$ is only $d$. Without loss of generality, it is reasonable to set $\lambda_{mn}|_{m\neq n} = 0$.

**Pure state**

The density matrix $\rho$ can be written as $\rho = |\Phi\rangle\langle\Phi|$ with the intended target entangled state $|\Phi\rangle = \sum_{m=1}^5 \lambda_m e^{i\theta_m}|\phi_m^A\rangle|\phi_m^B\rangle$. Here $\lambda_m = \sqrt{N'_m/\sum_m N'_m}$, $N'_m$ is the abbreviations of $N'_{mm}$ (an element of $\mathbf{N}'$), and $\theta_m$ is the phase. Based on the criterion in Eq. (4) of the main text, we can obtain a suitable transformation matrix $\mathbf{T}$ as

$$\mathbf{T} = \frac{1}{\sqrt{5}}\begin{bmatrix} 1 & 1 & 1 & 1 & -1 \\ 1 & 1 & 1 & -1 & 1 \\ 1 & 1 & -1 & 1 & 1 \\ 1 & -1 & 1 & 1 & 1 \\ -1 & 1 & 1 & 1 & 1 \end{bmatrix}. \tag{S8}$$

We can easily construct the second basis $\{|\varphi_m^X\rangle\}_{m=1,...,5}$ by Eq. (5) in the main text. Then we measure the coincidence counts matrix $\mathbf{N}''$ under the second product basis $\{|\varphi_m^A\rangle|\varphi_n^B\rangle\}_{m,n=1,...,5}$. Due to the symmetry of $\mathbf{N}''$, we need only measure the elements of $N''_{mn(n\geqslant m)}$ in experiment. We build from Eq. (6) in the main text a set of nonlinear equations as

$$\sum\nolimits_{m,n=1}^{5} \lambda_m \lambda_n e^{i\delta_{mn}} T^{\dagger}_{mk} T^{\dagger}_{ml} T_{kn} T_{ln} = \frac{N''_{kl}}{N''_{\mathrm{C}}}. \tag{S9}$$

where $N''_C = (2N''_{11} + \sum_{l(l>k)}^{5} \sum_{k=1}^{5} N''_{kl})/12$ is a normalized coefficient and $\delta_{mn} = \theta_n - \theta_m$. In fact, the phase information of the intended target entangled state $|\Phi\rangle$ is contained in the relative phase differences $\{0 \leq \delta\theta_{1n} \leq \pi\}_{n=2,..,5}$ which are calculated as

$$\delta_{12} = \arccos\left[(\gamma_1 + \gamma_2 + \gamma_3 + \gamma_6)/(4\lambda_1\lambda_2)\right], \tag{S10a}$$
$$\delta_{13} = \arccos\left[(\gamma_1 + \gamma_2 + \gamma_4 + \gamma_7)/(4\lambda_1\lambda_3)\right], \tag{S10b}$$
$$\delta_{14} = \arccos\left[(\gamma_1 + \gamma_3 + \gamma_4 + \gamma_9)/(4\lambda_1\lambda_4)\right], \tag{S10c}$$
$$\delta_{15} = \arccos\left[(\gamma_1 + \gamma_6 + \gamma_7 + \gamma_9)/(4\lambda_1\lambda_5)\right], \tag{S10d}$$

where $\gamma_{q(k,l)} = \frac{5}{2}\left(\frac{N''_{kl}}{N''_{\mathrm{C}}} - 1\right)$, and $q(k,l)$ are defined as $q(1,2) = 1$, $q(1,3) = 2$, $q(1,4) = 3$, $q(1,5) = 4$, $q(2,4) = 6$, $q(2,5) = 7$, and $q(3,5) = 9$.

**Mixed state**

The mixed state obtained by dephasing the maximally entangled target state $|\Phi\rangle$ can be written as

$$\begin{aligned}\rho(p) =& p|\Phi\rangle\langle\Phi| + (1-p)\sum\nolimits_{m}^{5} \lambda_m^2 |\phi_m^A\rangle|\phi_m^B\rangle\langle\phi_m^A|\langle\phi_m^B| \\ =& p\sum\nolimits_{\substack{m,n=1\\ m\neq n}}^{5} \lambda_m\lambda_n e^{i\delta_{mn}} |\phi_m^A\rangle|\phi_m^B\rangle\langle\phi_n^A|\langle\phi_n^B| + \frac{1}{5}\sum\nolimits_{m=1}^{5} \lambda_m^2 |\phi_m^A\rangle|\phi_m^B\rangle\langle\phi_m^A|\langle\phi_m^B|.\end{aligned} \tag{S11}$$

Here $p$ is the visibility with $0 \leq p \leq 1$. The criterion defined for searching the desired transformation matrix T can be used. The second basis can be obtained with Eq. (5) in the main text. Then the coincidence counts matrix $\mathbf{N}''$ can be measured with the global product basis $\{|\varphi_m^A\rangle|\varphi_n^B\rangle\}_{m,n=1,...,5}$. Based on $\mathbf{N}''$, a set of nonlinear equations, which is different from Eq. (S9), can be built as follows

$$p\sum\nolimits_{m,n=1}^{5} \lambda_m\lambda_n e^{i\delta_{mn}} T^{\dagger}_{mk} T^{\dagger}_{ml} T_{kn} T_{ln} + \frac{1-p}{25} = \frac{N''_{kl}}{N''_{\mathrm{C}}}. \tag{S12}$$

Then relative phase difference $\{0 \leq \delta_{1n} \leq \pi\}_{n=2,..,5}$ are calculated as

$$\delta_{12} = \arccos\left[\left(\gamma_1^p + \gamma_2^p + \gamma_3^p + \gamma_6^p\right)/(4\lambda_1\lambda_2)\right], \tag{S13a}$$
$$\delta_{13} = \arccos\left[\left(\gamma_1^p + \gamma_2^p + \gamma_4^p + \gamma_7^p\right)/(4\lambda_1\lambda_3)\right], \tag{S13b}$$
$$\delta_{14} = \arccos\left[\left(\gamma_1^p + \gamma_3^p + \gamma_4^p + \gamma_9^p\right)/(4\lambda_1\lambda_4)\right], \tag{S13c}$$
$$\delta_{15} = \arccos\left[\left(\gamma_1^p + \gamma_6^p + \gamma_7^p + \gamma_9^p\right)/(4\lambda_1\lambda_5)\right], \tag{S13d}$$

where $\gamma^p_{q(k,l)} = \frac{5}{2p}\left(\frac{N''_{kl}}{N''_C} - 1\right)$.

Due to the presence of the visibility $p$, the 4 independent sub-equations in Eq. (S13) are not enough to determine the 4 unknown phases $\{\delta_{1n}\}_{n=2,..,5}$ and the visibility $p$. In principle, we need to build only one independent sub-equation again, we can completely determine $\{\delta_{1n}\}_{n=2,..,5}$ and $p$. Therefore, we need to construct the third basis and then to measure coincidence counts matrix under this basis. Similarly, with the criterion in Eq. (4) of the main text, we can obtain another suitable transformation matrix $\mathbf{T}'$ and construct the third basis as

$$\begin{bmatrix} |\psi_1^{A/B}\rangle \\ |\psi_2^{A/B}\rangle \\ |\psi_3^{A/B}\rangle \\ |\psi_4^{A/B}\rangle \\ |\psi_5^{A/B}\rangle \end{bmatrix} \propto \mathbf{T}' \begin{bmatrix} |\phi_1^{A/B}\rangle \\ |\phi_2^{A/B}\rangle \\ |\phi_3^{A/B}\rangle \\ |\phi_4^{A/B}\rangle \\ |\phi_5^{A/B}\rangle \end{bmatrix}, \quad \text{with } \mathbf{T}' = \frac{1}{\sqrt{5}} \begin{bmatrix} 1 & 1 & 1 & 1 & i \\ 1 & 1 & 1 & i & 1 \\ 1 & 1 & i & 1 & 1 \\ 1 & i & 1 & 1 & 1 \\ i & 1 & 1 & 1 & 1 \end{bmatrix}. \tag{S14}$$

After we measure the coincidence counts $\mathbf{N}'''$ under the third product basis $\{|\psi_m^A\rangle|\psi_n^B\rangle\}_{m,n=1,...,5}$, another set of nonlinear equations can be built as

$$p\sum\nolimits_{m,n=1}^{5} \lambda_m\lambda_n e^{i\delta_{mn}} T'^{\dagger}_{mk} T'^{\dagger}_{ml} T'_{kn} T'_{ln} + \frac{1-p}{25} = \frac{N'''_{kl}}{N'''_{\mathrm{C}}}, \tag{S15}$$

where $N'''_{kl}$ is an element of $\mathbf{N}'''$ and $N'''_{\mathrm{C}}$ is a normalized coefficient.

In fact, to build the 5th independent sub-equation, we do not need to measure all the $(d^2+d)/2 = 15$ independent elements in $\mathbf{N}'''$. We only need to measure two larger matrix elements in $\mathbf{N}'''$, which are defined as $N'''_{pq}$ and $N'''_{uv}$. Thus, with Eq. (S15), we can build the 5th independent sub-equation as follows

$$\frac{p\sum_{m,n=1}^{5} \lambda_m\lambda_n e^{i\delta_{mn}} T'^{\dagger}_{mk} T'^{\dagger}_{ml} T'_{kn} T'_{ln} + (1-p)/25}{p\sum_{m,n=1}^{5} \lambda_m\lambda_n e^{i\delta_{mn}} T'^{\dagger}_{mu} T'^{\dagger}_{mv} T'_{un} T'_{vn} + (1-p)/25} = \frac{N'''_{kl}}{N'''_{uv}}, \tag{S16}$$

Finally, by solving the selected 4 sub-equations in Eq. (S13) and Eq. (S16) together, we can aquire all the phase $\{\theta_m\}$ and the visibility $p$ completely. So, compared with the pure state, only a few measurements are needed to be added for tomography of the mixed HD entangled state.

## VII. ALT FOR MULTI-PARTITE HIGH-DIMENSIONAL ENTANGLEMENT

We extend our ALT method into multi-partite HD entangled state. Here we develope our ALT method for pure state only. A pure multi-partite HD entangled state $|\Phi\rangle$ can be written as

$$|\Phi\rangle = \sum_{m_1=1}^{d_1}\sum_{m_2=1}^{d_2}\cdots\sum_{m_n=1}^{d_n} \lambda_{m_1m_2...m_n} e^{i\theta_{m_1m_2...m_n}} |\phi_{m_1}^{P_1}\rangle|\phi_{m_2}^{P_2}\rangle\cdots|\phi_{m_n}^{P_n}\rangle, \tag{S17}$$

where $P_j$ indicates the $j$th particle among $n$ particles and $d_j$ represents the dimension of the $j$th particle. $\theta_{m_1m_2...m_n}$ and $\lambda_{m_1m_2...m_n}$ are the phase and amplitude of $|\phi_{m_1}^{P_1}\rangle|\phi_{m_2}^{P_2}\rangle\cdots|\phi_{m_n}^{P_n}\rangle$, respectively, and satisfies $\sum_{m_1=1}^{d_1}\sum_{m_2=1}^{d_2}\cdots\sum_{m_n=1}^{d_n}\lambda^2_{m_1m_2\cdots m_n} = 1$. $\{|\phi_{m_j}^{P_j}\rangle\}$ represents the first basis. We project $|\Phi\rangle$ into the first basis $|\phi_{m_1}^{P_1}\rangle|\phi_{m_2}^{P_2}\rangle\cdots|\phi_{m_n}^{P_n}\rangle$ to measure the coincidence counts $N'_{m_1m_2...m_n}$ and obtain $\lambda_{m_1m_2...m_n}$

$$\lambda_{m_1m_2...m_n} = \sqrt{\frac{N'_{m_1m_2...m_n}}{\sum_{m_1,m_2,...,m_n} N'_{m_1m_2...m_n}}}. \tag{S18}$$

Thus we can search the suitable transformation matrix $\mathbf{T}^{P_j}$ for the particle $P_j$, and $\mathbf{T}^{P_j}$ must also satisfy the criterion in Eq. (4) of the main text. Then we build the second basis as $|\varphi_{m_j}^{P_j}\rangle = \sum_{m'_j}^{d_j} T^{P_j}_{m_jm'_j}|\phi_{m'_j}^{P_j}\rangle$. By projecting $|\Phi\rangle$ into the basis $|\varphi_{m_1}^{P_1}\rangle|\varphi_{m_2}^{P_2}\rangle\cdots|\varphi_{m_n}^{P_n}\rangle$, the coincidence $N''_{m_1,m_2,...,m_n}$ is counted and used to establish $d_1\times d_2\times ...\times d_n$ nonlinear equations as follows

$$\left|\sum_{m_1=1}^{d_1}\sum_{m_2=1}^{d_2}\cdots\sum_{m_n=1}^{d_n}\sqrt{\frac{N'_{m_1m_2...m_n}}{\sum_{m_1,m_2,...,m_n} N'_{m_1m_2...m_n}}}\left(T^{P_1}_{m_1m'_1}\right)^{\dagger}\left(T^{P_2}_{m_2m'_2}\right)^{\dagger}\cdots\left(T^{P_n}_{m_nm'_n}\right)^{\dagger} e^{i\theta_{m_1m_2...m_n}}\right|^2 = \frac{N''_{m'_1m'_2...m'_n}}{N''_{\mathrm{C}}}. \tag{S19}$$

By solving Eq. (S19), all the phases $\{\theta_{m_1m_2...m_n}\}$ can be obtianed completely. Finally, the density matrix can be calculated with $\rho = |\Phi\rangle\langle\Phi|$ and the tomography of the multi-partite HD entangled state has been realized.